Analyzing the Impact of Current Flow on Defect Detection in Various Samples Using Magnetic Particle Inspection

Hasan Abdulsahib Mezaal Omar Yaseen Saeed
Scientific Research Commission. Baghdad/ Iraq
E-mail: hasan.a.mezaal@src.edu.iq

Abstract

Magnetic Particle Inspection (MPI) is a widely used as non-destructive testing method for detecting surface and near-surface discontinuities in ferromagnetic materials. It is highly effective in identifying cracks, laps, and other flaws that may not be visible to the naked eye. This research investigates the influence of electric current on defect detection within four metallic samples of different geometries. The evaluation employs magnetic particle inspection (MPI) to assess surface-level flaws deliberately introduced with varying dimensions and spacing. A bench-type machine generates an alternating current through dual magnetic poles, while a fluorescent magnetic suspension is applied to reveal defect indications. The electric current is progressively elevated to examine its role in enhancing or limiting defect visibility across the tested specimens. The result shows highly effect of sample engineering shape, defect depth and size on testing result.

Keywords: Magnetic Particle Inspection, Non-Destructive Testing, Defect Detection, fluorescent, discontinuities.

تحليل تأثير تدفق التيار على كشف العيوب في عينات مختلفة باستخدام فحص الجسيمات المغناطيسية

حسن عبد الصاحب مزعل عمر ياسين سعيد
هيئة البحث العلمي ، بغداد ، العراق

الخلاصة

يُعد فحص الجسيمات المغناطيسية (MPI) من الطرق واسعة الاستخدام في الاختبارات غير الإتلافية للكشف عن العيوب السطحية والقريبة من السطح في المواد ذات الخواص المغناطيسية. ويُعد هذا الأسلوب فعالاً للغاية في تحديد الشقوق والطيات والعيوب الأخرى التي قد لا تكون مرئية للعين المجردة. يتناول هذا البحث دراسة تأثير التيار الكهربائي على عملية كشف العيوب في أربعة نماذج معدنية ذات أشكال هندسية مختلفة. استخدم فحص الجسيمات المغناطيسية (MPI) لتقييم العيوب السطحية التي أُدخلت عمدًا بأبعاد ومسافات متباينة. حيث تولد آلة مخبرية تيارًا متناوبًا عبر قطبين مغناطيسيين، بينما استخدم تعليق مغناطيسي فلوري لإظهار مؤشرات العيوب. فضلا عن ذلك رفعت شدة التيار الكهربائي تدريجيًا لدراسة دوره في تحسين أو تقليل وضوح العيوب في العينات المختبرة. النتائج أظهرت النتائج تأثير عالي لشكل العينة الهندسي، عمق العيب وحجمه على نتائج الفحص.

الكلمات المفتاحية: الفحص بالجسيمات المغناطيسية ، الفحوصات اللاتلافية ، اكتشاف العيب ، فلورة ، الانقطاعات.

1-Introduction

Ensuring the integrity of mechanical parts is crucial for the reliability and safety of engineering systems. Defects such as cracks, holes, and general discontinuities can affect the performance of components like shafts in DC motors, leading to significant quality and safety issues. Detecting these defects before they result in failure is essential. Traditional destructive testing methods, including tensile, flexural, and torsion tests, often damage or destroy the parts being tested, making them unsuitable for components that must remain in service (Hellier, 2012).

Non-Destructive Testing (NDT) methods offer a valuable alternative, allowing for the detection of flaws without harming the part. Among these methods, Magnetic Particle Inspection (MPI) is particularly effective for identifying surface and shallow subsurface defects in ferritic metals. MPI works by applying a magnetic field to the part and using magnetic particles to detect discontinuities. These particles gather at points of magnetic flux leakage, which occurs at the sites of defects, making them visible to inspectors (Cartz, 1995).

The importance of MPI in various industries cannot be overstated. From automotive and aerospace to manufacturing and power generation, ensuring the structural integrity of components is paramount. MPI is preferred for its sensitivity, speed, and cost-effectiveness, making it an essential tool for maintaining high safety and quality standards. Despite its widespread use, understanding the principles of MPI, such as the effects of current flow on defect detection, remains an area ripe for exploration, (Gupts, 2021).

This study focuses on analyzing the impact of varying current flow on the detection of defects in different sample shapes using MPI. Four samples, each with distinct dimensions and defect characteristics, were subjected to increasing levels of AC current to observe how it affects defect visibility. The samples, manufactured in scientific research committee, were tested using both the rigid coil technique and the threaded bar method. By gradually increasing the current and applying fluorescent magnetic particles under ultraviolet light, (Iowa University, 2024)

The current flow can influence the formation of the magnetic field and, consequently, the visibility of defects. The depth and orientation of flaws, as well as the geometry and material properties of the samples, play critical roles in the detection process. By systematically studying these parameters, the research seeks to provide insights into optimizing MPI procedures. Furthermore, the study addresses practical challenges faced in industrial applications. For instance, components with complex geometries or those exposed to varying operational stresses may exhibit defects that are difficult to detect using standard MPI techniques. The findings of this research aim to enhance the reliability of MPI, offering more robust and adaptable inspection protocols that can be applied across different sectors, (Wu, *et al*, 2024).

Li, *et al*, (2020). studied how magnetic particles behave during crack detection using fluorescent magnetic particle inspection (MPI). They developed a mathematical model to understand the forces acting on the particles near a surface crack, and used

MATLAB to calculate the distance where particles can still be attracted by the magnetic field. Their experiments showed that when the particle concentration is too low or too high, the crack image becomes unclear. They found that a concentration of 3–4 mL/L gives the best contrast between the crack and the background, which helps in improving automatic detection systems.

Sacarea, *et al* (2021), worked on improving the way of Magnetic Particle Inspection (MPI), especially for cylindrical metal parts. In this study, they explained how traditional methods often depend too much on the inspector, which can lead to mistakes or missing small cracks. To solve this, they introduced a new setup that helps create a more stable magnetic field around the part. This makes it easier to see defects without needing to move the part multiple times. The device they designed also helps keep the part properly aligned, reducing the need for repeated testing. Sacarea's group tested their method under real conditions and found that inspection became faster and more accurate. Their results showed that using this device can make the magnetic testing process more reliable and save time.

Bowler, (2002). created a mathematical model that shows how the magnetic field changes when a crack is present. they used a special technique called "conformal mapping" to turn the complex shape of a crack into a simpler form. This helped them get accurate results without needing a high technique computer simulation. Bowler's team looked at different crack shapes—like narrow cracks and semi-elliptical ones—and calculated the strength of the magnetic field near the crack open. Their results showed how magnetic particles are affected by the field, which helps in making MPI more accurate.

Yang, *et al*, (2022). introduced an automated method to detect surface cracks in bearing rings during magnetic particle inspection, which is usually done manually. The researchers focused on handling complex image backgrounds that often confuse traditional detection methods. Their approach involves two main steps: first, identifying likely defect areas by demonstrating how the human eye spots line-like patterns using grayscale and geometric cues; and second, using a customized lightweight deep learning model (MobileNetV3 enhanced with coordinate-based attention) to confirm if those areas contain real cracks. The method achieved high precision and speed, showing strong potential for real-world industrial use.

Tao, et al, (2016) worked on making Magnetic Particle Inspection (MPI) smarter by using a machine vision system. the main goal was to improve how railway wheelsets are tested using fluorescent magnetic particles, which helps in finding cracks or damage more easily. By combined traditional MPI with a camera and image processing system. This allowed to automatically detect the bright spots where particles gather—these spots usually mean there's a crack or defect. The system can also show the results on a screen, which helps the inspector see everything clearly without guessing. What's special about this work is that it reduces the need for manual judgment. The

computer can look at the image and tell if there is a problem. This makes the process more accurate and less dependent on how skilled the inspector is.

Zolfaghari, *et al*, (2018) investigated how reliable and sensitive magnetic particle testing (MT) is when used to find surface cracks in welded parts. Instead of using fake cracks, they picked real welding cracks to get more accurate results. They first examined the cracks under a microscope to measure their exact sizes, then tested the same parts using manual magnetic particle inspection. The goal was to see which cracks the method could find and which it missed. After comparing both sets of results, they calculated those cracks shorter than 1.5 mm were often missed, but cracks larger than 2.5 mm were always detected. The study also used probability curves to estimate how likely it is to find cracks based on their length. Their findings give useful guidelines for engineers to know when this method is effective and when it might miss small defects.

2- Methodology

2-1 Magnetization

Magnetization is a fundamental process in non-destructive testing (NDT) used to identify surface and near-surface discontinuities, such as cracks, in ferromagnetic materials. The principle behind this technique is to introduce a magnetic field into the material, which, when encountering a discontinuity, creates a leakage field detectable at the surface. The magnetic particles applied to the surface of the material are attracted to these leakage fields, forming a visible indication of the flaw.

For effective detection, the magnetizing field lines must be oriented in such a way that they intersect the discontinuity. This intersection is crucial because it results in a leakage

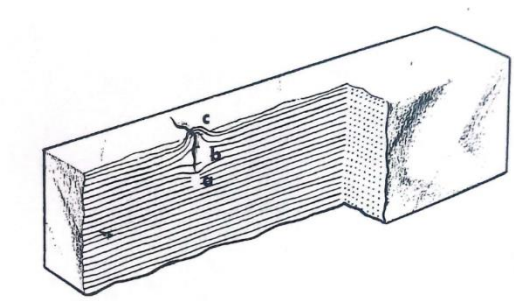

field that extends into the air above the crack, making the discontinuity visible when magnetic particles are applied. The leakage field occurs across the crack and around its edges from the bottom as labeled (c, b, a) respectively, as shown in Figure (1)(Betz, 1967).

Figure 1 Field leakage at discontinuity (an around the discontinuity, b across the discontinuity, c above the discontinuity).

The orientation of the magnetic field relative to the flaw is a critical factor in the magnetization process. For optimal detection, the field lines should be either perpendicular to the flaw or within a 45° angle to it. This orientation ensures the strongest possible leakage field, enhancing the visibility of the discontinuity. There are two primary methods used to achieve this optimal orientation.

2-1-1 Threaded bar or cable technique:

This technique involves passing a conductive bar or cable through the bore or aperture of the specimen being tested. Figures (2) and (3) illustrate how the magnetic field is induced around the bar or cable, effectively magnetizing the specimen.

This approach is particularly useful for detecting flaws in cylindrical or hollow specimens, where direct magnetic flow may not be feasible.

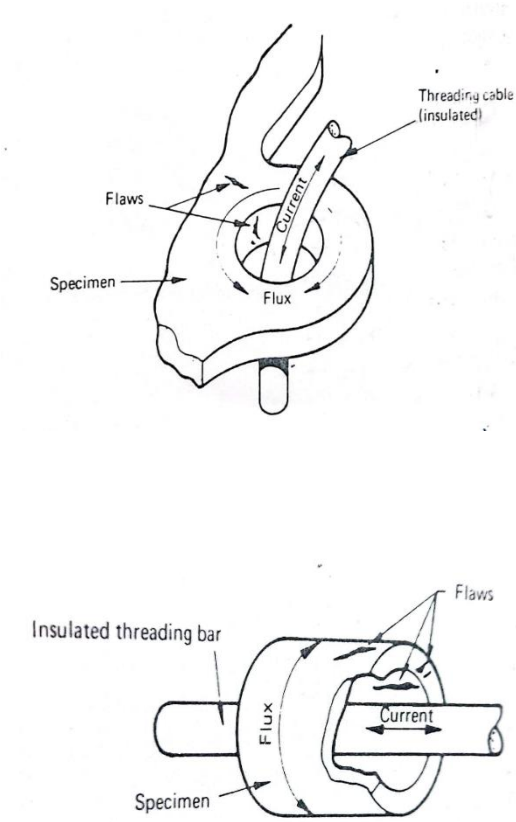

Figure 2 Threaded bar (cable) technique

Figure 3 Threading bar technique

This technique involves placing the specimen inside a rigid coil, which consists of several windings. As shown in Figure 4, the coil generates a uniform magnetic field around the specimen. This method is advantageous for testing irregularly shaped specimens or when a consistent magnetic field is required across the entire surface. The rigid coil technique allows for the detection of flaws that may not be accessible through other magnetization methods.

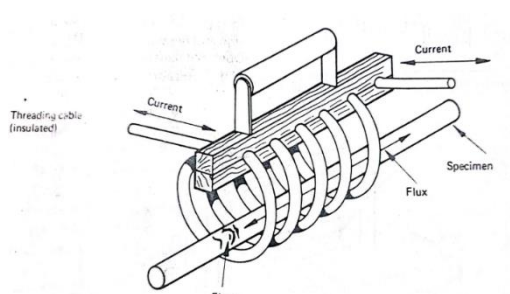

Figure 4 Rigid coil technique

The choice of magnetization method depends on several factors, including the shape and size of the specimen, the expected orientation of the flaws, and the specific requirements of the inspection process. Each method offers unique benefits and challenges, and understanding these is essential for accurate and reliable flaw detection in ferromagnetic materials. By selecting the appropriate magnetization technique, inspectors can ensure the integrity and safety of critical components in various industrial applications BSI (1981).

2.2 Detecting defects

After the specimen has been thoroughly cleaned of any dust and rust and properly magnetized, the next critical step in the non-destructive testing process is the application of ferritic particles. These particles can be applied in two main forms: as a dry powder or as a suspension in a liquid. The choice between these forms depends on the specific requirements of the inspection and the nature of the specimen.

Once applied, these particles gather around the leakage field created by the discontinuity in the magnetized specimen. This occurs because the magnetic field at the site of the flaw disturbs the uniform magnetic flux, causing a portion of the field to leak into the surrounding air. The ferritic particles are drawn to these areas of increased magnetic flux density, accumulating around the discontinuity and making it visible to the naked eye.

To ensure the visibility of the flaw indications, it is essential to maintain an appropriate level of illumination. The recommended light level for observing the gathered particles is not less than

500 lux. Adequate lighting allows the inspector to clearly see the accumulation of particles and accurately identify any potential defects, BSI (1981).

In some cases, particularly when enhanced visibility is required, a fluorescent ink powder is applied. This technique is beneficial as it provides a high contrast between the detecting medium and the specimen under test, making it easier to spot flaws. When using fluorescent particles, the testing environment must be carefully controlled. The room should be darkened, with ambient light levels not exceeding 10 lux. This low-light environment is crucial for the effectiveness of the fluorescent particles, which emit a bright glow under ultraviolet (UV) light. The application of UV light causes the fluorescent particles to fluoresce, highlighting the flaws in stark contrast against the dark background of the specimen, Lau, (2022).

The choice of using fluorescent particles over conventional methods depends on several factors, including the complexity of the specimen's geometry, the required sensitivity of the inspection, and the type of flaw being investigated. This technique is particularly advantageous when inspecting complex components where subtle indications may be missed under normal lighting conditions.

Overall, the detection phase is a vital part of the magnetic particle testing process. It involves careful preparation and execution to ensure accurate identification of flaws. By selecting the appropriate particle type and ensuring optimal lighting conditions, inspectors can achieve high precision in identifying discontinuities, thereby maintaining the integrity and safety of critical components in various industrial applications, Magnaflux, (2011).

2-3 Equations

a. Ampère's Circuital Law For the bench machine with pole pieces separated by an effective magnetic path length ℓ, the magnetic field intensity H in the sample is given by

$$\oint_{\mathcalC} \mathbfH \cdot d\mathbf\ell = I_{\rmenc} \quad \Rightarrow \quad H = \fracI\ell$$

$$\fracI\ell \quad (1)$$

where

- I is the applied AC current (A).
- ℓ is the mean magnetic path length between poles (m).

b. Magnetic Flux Density The resulting magnetic flux density B in the ferromagnetic sample is

$$B = \mu_0 \mu_r H = \mu_0 \mu_r \frac{I}{\ell} \quad (2)$$

where

- $\mu_0 \approx 4\pi \times 10^{-7} \frac{\mathrm{H}}{\mathrm{m}}$ is the permeability of free space,
- μ_r is the relative permeability of the sample material.

c. Leakage Flux at a Surface-Break Defect A surface-breaking crack of width w and depth δ interrupts the flux path, creating a leakage flux $\Phi_{\rmleak}$. A first-order estimate is

$$\Phi_{\rmleak} \approx B\, w\, \delta = \mu_0 \mu_r \fracI\ell\, w\, \delta \quad (3)$$

where

- w is the defect opening width (m).
- δ is the defect depth (m).

d. Magnetic Force on a Particle A magnetic particle of volume V_p and

susceptibility χ_p in a non-uniform field experiences a force

$$\mathbf{F} = V_p \frac{\chi_p}{\mu_0} (\mathbf{B} \cdot \nabla)\mathbf{B} \quad \Rightarrow \quad F_x \approx V_p \frac{\chi_p}{\mu_0} B \frac{\partial B}{\partial x} \quad (4)$$

Detection occurs when this force exceeds the particle's weight mg.

e. Detection Threshold Requiring $F_x \geq mg$ gives a minimum flux density $B_{\backslash rmth}$:

$$V_p \backslash frac\chi_p\mu_0 B_{\backslash rmth} \backslash frac\partial B\partial x \geq m\,g \implies B_{\backslash rmth} \approx \sqrt{\backslash fracm\,g\,\mu_0 V_p\,\chi_p\,\kappa} \quad (5)$$

where κ represents a characteristic field gradient $\frac{\partial B}{\partial x}$.

The corresponding **minimum current** $I_{\min}$ needed is

$$I_{\backslash min} = \backslash frac\ell\mu_0\,\mu_r\,B_{\backslash rmth} = \backslash frac\ell\mu_0\,\mu_r \sqrt{\backslash fracm\,g\,\mu_0 V_p\,\chi_p\,\kappa} \quad (6)$$

f. Empirical Detection Probability To fit your experimental data, you might introduce an empirical detection-probability curve P_d as a function of applied current:

$$P_d(I) = \frac{1}{1+\exp[-\alpha\,(I-I_{50})]} \quad (7)$$

where

- I_{50} is the current giving 50 % detection probability.
- α is a steepness parameter determined by regression.

Abbreviations:

Symbol	Definition
I	Applied AC current (A)
ℓ	Magnetic path length between pole pieces (m)
H	Magnetic field intensity (A/m)
B	Magnetic flux density (T)
μ_0	Permeability of free space (H/m)
μ_r	Relative permeability of sample
w, δ	Defect opening width and depth (m)
$\Phi_{\backslash rmleak}$	Leakage flux through defect (Wb)
V_p	Volume of a magnetic particle (m^3)
χ_p	Magnetic susceptibility of particle
m	Mass of magnetic particle (kg)
g	Gravitational acceleration (9.81 $\frac{m}{s^2}$)
κ	Characteristic $\frac{\partial B}{\partial x}$ (T/m)
P_d	Defect detection probability (unitless)
I_{50}, α	Parameters of the logistic detection model

3- Experimental work

The experimental work completely depends on BSI BS 6072: 1981. in this paper four samples were used as shown in Table (1)

Table 1 . Details of samples and defects

Defect ID	Sample	Sample Shape	Sample Dimensions mm^3	Defect Diameter (mm)	Defect Depth (mm)	Detection Current (A)	Detection
D1	Sample 1	Rectangular Cross section	375×20×20	1	1	350	Yes
D2	Sample 2	Rectangular Cross section	200×25×25	0.6	0.5	200	Yes
D3				0.6	2	765	Yes
D4				0.6	3	900	Yes
D5				0.6	5		No
D6	Sample 3	Circular Cross section	Ø200	1	1	400	Yes
D7				1	2	900	Yes
D8				1	3		No
D9	Sample 4	Circular Cross section	Ø125	2	0.5	200	Yes
D10				2	2	350	Yes
D11				2	3	790	Yes
D12				2	5		No

All samples drilled to produce the defects with various diameters and depths as shown in Table (1). Current bench machine was used to generate current flow for all samples. Before doing the tests, all samples were cleaned from dust and rust, demagnetized by the demagnetizer device and check if there is a residual magnetic field on samples by using gauss meter. The first and second samples tested by using rigid coil technique as shown in Figure (5) and Figure (6) respectively. The third and fourth sample tested by using threaded bar method as shown in Figure (7) and Figure (8) respectively. After putting the threaded bar or rigid coil between the bench machine poles gently increase the current from 0 to 1000 Ampere with spraying the fluorescent magnet particles on the sample while supposing ultraviolet light on the sample at dark room until all possible defect shown.

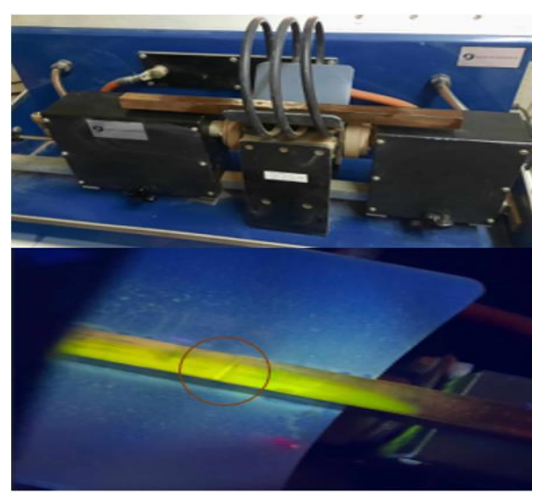

Figure 5 Sample 1 under test

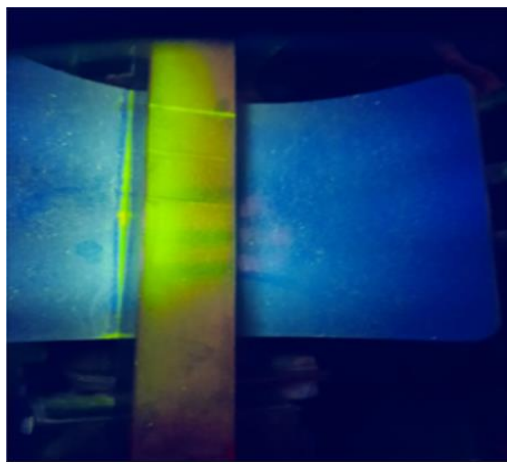

Figure 6 Sample 2 under test

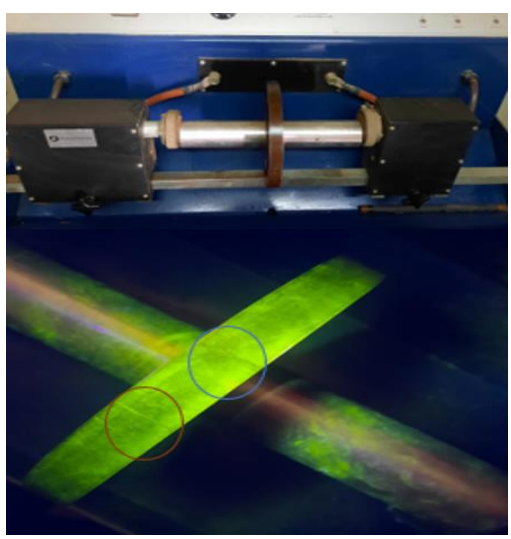

Figure 7 Sample 3 under test

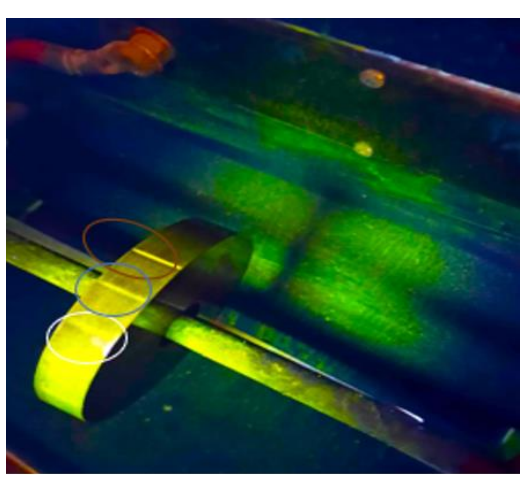

Figure 8 Sample 4 under test

4- Results and Discussions

This section presents analysis of the defect-detection results obtained from all tested ferromagnetic samples. Three main factors were discussed: defect depth, defect diameter, and the geometric shape of the sample. The performance of defect detection was assessed based on the minimum current required to reveal indications using fluorescent magnetic particles.

Depending on the value of supplying current the capability of defects detecting was compared. The result of this work has been documented by using real time photos during the experimental work and by using clarifying tables and Figures. As shown in Figure (5) the particles gathered on defect in sample one and cycled in red. In sample (2) just three defects make the particles gathered as seen in Figure (6) in different quantities and cycled in red, blue and white respectively referred to previous sector that mentions the size and depth of defects. the particles in sample three and four gathered in different quantities too depending on defects size and depth and size of samples as seen in Figure (7) and Figure (8) respectively.

4-1 The effect of defect diameter and depth

Table (2) summarizes the combined influence of defect depth and diameter on detectability. Defects with depths between 0.5 and 2 mm were successfully detected for most diameter values, depending on sample geometry. At a depth of 3 mm, missed indications begin to appear, particularly for small defect diameters. At 5 mm depth, none of the defects were detected, confirming that excessive depth causes severe magnetic flux dispersion and suppresses surface leakage. The (✓) mark means

the defect is detected, (✕) mark means the failure of detecting and mark (‒) means that the specific defect size/depth combination was not present in samples.

Table 2 . Detecting ability of defect

Depth \ defect Diameter	0.6 mm	1.0 mm	2.0 mm
0.5 mm	✓	-	✓
1.0 mm	✓	✓	-
2.0 mm	✓	✓	✓
3.0 mm	✓	✕	✓
5.0 mm	✕	✕	✕

4-2 The relationship between current and defect Characteristics

To analyze the quantitative relationship between the applied current and defect characteristics, the data in Table (3) below highlights the specific current levels required to detect each defect type.

Table3.Correlation between defect characteristics and detection current

Defect Depth (mm)	Defect Diameter (mm)	Detection Current (A)	Shape of sample	Sample Dimensions (mm^3)	Samples
0.5	0.6	200	Rectangular	200×25×25	Sample 2
0.5	2	200	Circular	Ø125	Sample 4
1	1	350	Rectangular	375×20×20	Sample 1
1	1	400	Circular	Ø200	Sample 3
2	0.6	765	Rectangular	200×25×25	Sample 2
2	2	350	Circular	Ø125	Sample 4
2	1	900	Circular	Ø200	Sample 3
3	0.6	900	Rectangular	200×25×25	Sample 2
3	2	790	Circular	Ø125	Sample 4
Average current = Sum of detecting current / 9 = 540 A					

Based on these data in Table (3) we generated scatter plots to visualize the trends. Figure (9) illustrates the relationship between defect diameter and detection current so that larger defect diameters generally require lower detection currents, while smaller diameters are associated with higher current levels , while Figure (10) shows the relationship between defect depth and current demonstrating the opposite trend with depth: deeper defects demand significantly higher currents to generate visible indication.

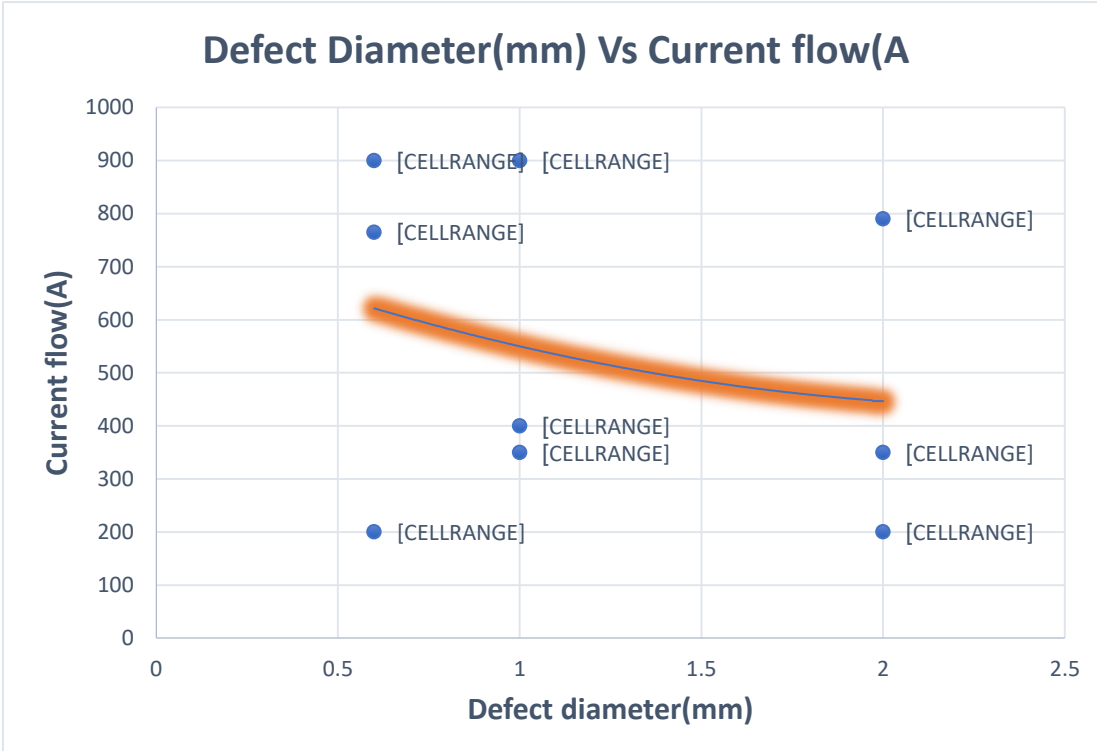

Figure 9 Relationship between defect diameter and detection current

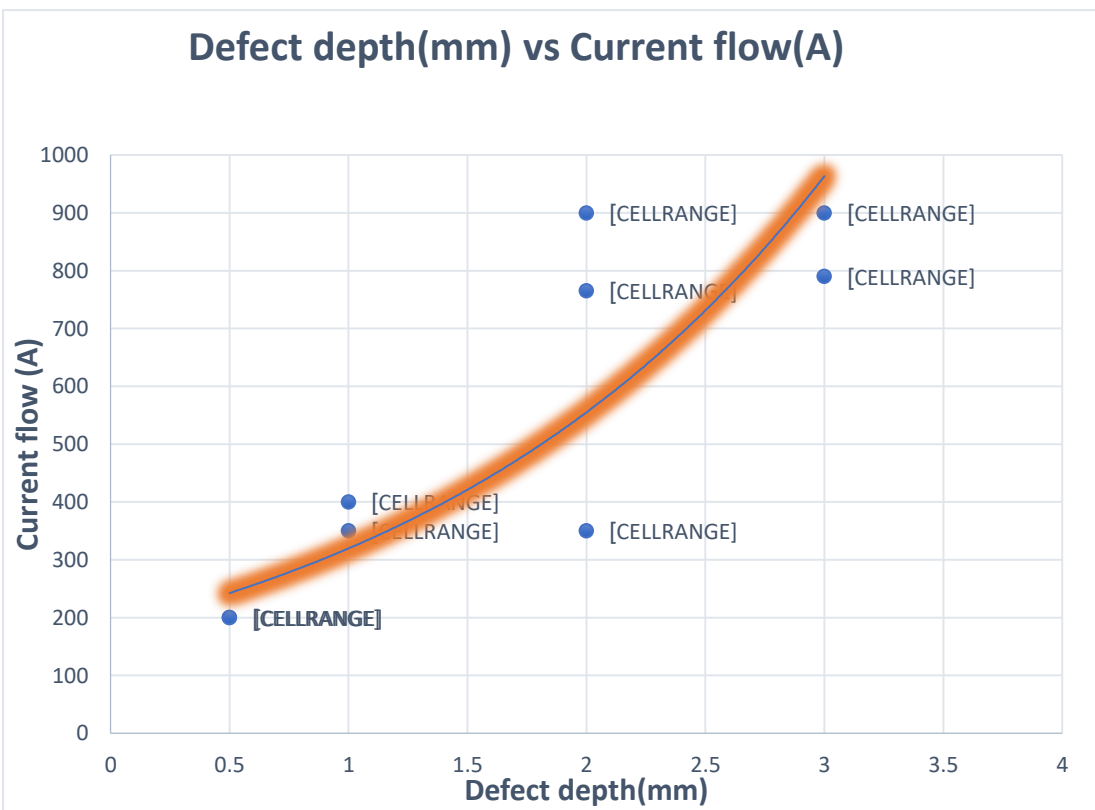

Figure 10 Relationship between defect depth and current

The experimental results shown in Tables (1,2,3) and the trends observed in Figures 9 and 10 are governed by the fundamental physics of magnetic particle inspection, as described by the mathematical model in the methodology :

1. Magnetic Field Generation: The need to increase current for certain samples is primarily governed by Equation (1) and Equation (2). Since the magnetic flux density *(B)* is directly proportional to the applied current (*I*), increasing the current is the primary method to boost the magnetic field strength necessary to penetrate the material and energize the discontinuity, and create a detectable flux leakage at the surface.
2. Effect of Defect Diameter: The downward trend in Figure (9) (where larger defects require less current as shown in sample 4) is explained by Equation (3) $\Phi_{\backslash rmleak} \approx B\, w\, \delta = \mu_0\, \mu_r \backslash fracI\ell\, w\, \delta$ The leakage flux ($\Phi_{\backslash rmleak}$) is directly proportional to the defect width or diameter . Consequently, a defect with a larger diameter naturally creates a massive disruption in the magnetic path and a stronger leakage field. Therefore, a relatively low current (and lower flux density) is sufficient to produce a visible indication, unlike smaller defects which require high currents to force a detectable leakage.
3. Effect of Defect Depth: Conversely, the sharp increase in current required for deeper defects shown in Figure 10 is due to magnetic flux dispersion. As the defect depth increases, the magnetic field gradient at the surface becomes weaker and more diffuse. To compensate for this loss of intensity at the surface, the applied current must be increased significantly to push the flux density beyond the detection threshold.
4. Sample Geometry: The variation in results between sample shapes (e.g., Sample 3 vs. Sample 4) is attributed to the magnetic path length as shown in Equation (1). Larger samples have a longer magnetic path, leading to higher magnetic reluctance. This requires a higher magnetizing current to achieve the same flux density compared to smaller sample.
5. Particle Adhesion Threshold: According to Equations (4) $\mathbf{F} = V_p \frac{\chi_p}{\mu_0} (\mathbf{B} \cdot \nabla)\mathbf{B} \quad \Rightarrow \quad F_x \approx V_p \frac{\chi_p}{\mu_0} B \frac{\partial B}{\partial x}$ and (5) $V_p \backslash fracχ_p\mu_0\, B_{\backslash rmth} \backslash frac\partial B\partial x \geq m\, g \implies B_{\backslash rmth} \approx \sqrt{\backslash fracm\, g\, \mu_0 V_p\, \chi_p\, \kappa}$, particle indication occurs only when the magnetic force acting on the particle exceeds its weight. The "No" detections recorded for 5 mm–deep defects (Table 2) indicate that, even at maximum applied current, the resulting flux leakage was too weak to generate sufficient magnetic force to hold the particles in place. This confirms that deep defects (>3 mm) fall below the particle adhesion threshold under the available testing conditions.

5- Conclusions and future work

From the experiments and results of this study, we can conclude the following:

1- Current vs. Defect: The results clearly show that deep defects need more current to be detected. On the other hand, large defects (wide diameter) are easier to find and require less current.

2- Sample Shape: The size and shape of the sample play a big role in testing. We found that larger samples weaken the magnetic field because of dispersion, so they need a higher current compared to smaller samples.

3- Detection Limit: Finding defects that are deeper than 3 mm is very difficult. If the defect is 5 mm deep, it cannot be detected at all because the magnetic leakage at the surface becomes too weak.

4- Best Current Value: We found that 540 Amperes is the best average setting. It is a "balance point" that detects most defects without wasting too much power. This value can be used as a starting point for future tests.

- Future Work: For future research, we suggest the following:
a- Testing samples with more complex and irregular shapes to see how the current behaves.

b- Using computer programs like MATLAB or Python to simulate the test before doing it. This helps in finding the right settings (like current amount) faster and more accurately.

6 – Acknowledgment

The authors would like to express their sincere gratitude to the Scientific Research Commission in Iraq for their general support. We are also deeply grateful to the Department of Engineering Support and Services, specifically the laboratories of the Engineering Inspection Division, for providing the necessary facilities and equipment to complete the experimental part of this research.

7- References

-**Betz**, C. E. (1967). *Principles of magnetic particle testing*. Magnaflux Corp. Principles of magnetic particle testing by Carl E. Betz | Open Library.

-**Bowler**, J. R. (2002). Evaluation of the magnetic field near a crack with application to magnetic particle inspection. *Journal of Physics D: Applied Physics, 35*(18), 2237–2242. https://doi.org/10.1088/0022-3727/35/18/301

-**British Standards Institution**. (1981). *Method for magnetic particle flaw detection (BS 6072:1981).* https://codehub.building.govt.nz/assets/_generated_pdfs/bs-60721981-5619.pdf

-**Cartz**, L. (1995). *Nondestructive testing* (1st ed.). ASM International. ISBN: 9780871705174

-**Gupta**, M., & Khan, M. A. (2021). Advances in applications of non-destructive testing (NDT): A review. *International Research Journal of Engineering, IT & Science Research, 7*(3), 76–86. https://sloap.org/journals/index.php/irjeis/article/view/1003

-**Hellier**, C. J. (2012). *Handbook of nondestructive evaluation* (2nd ed.). McGraw-Hill. ISBN: 9780071777148.

-**Iowa State University Center for Nondestructive Evaluation**. (n.d.). Nondestructive evaluation techniques: Magnetic particle. Retrieved May 27, 2024, https://www.nde-ed.org/NDETechniques/MagneticParticle/index.xhtml

-**Lau**, S. (2022). *Reducing measurement error in magnetic particle inspection through the optimization of process parameters and artificially intelligent solutions* [Doctoral dissertation, Iowa State University]. Iowa State University. https://www.imse.iastate.edu/files/2023/05/Lau_iastate_0097E_20280.pdf

-**Li**, L., Yang, Y., Cai, X., & Kang, Y. (2020). Investigation on the formation mechanism of crack indications and the influences of related parameters in magnetic particle inspection. *Applied Sciences, 10*(19), 6805. https://doi.org/10.3390/app10196805

-**Magnaflux Corp**. (2011). *Magnetic particle inspection reference guide.* https://magnaflux.com/Files/Instructions/Magnetic-Particle-Inspection_Reference-Guide.pdf

-**Sacarea**, A. I., Oancea, G., & Parv, L. (2021). Magnetic particle inspection optimization solution within the frame of NDT 4.0. *Processes, 9*(6), 1067. https://doi.org/10.3390/pr9061067

-**Tao**, M., Sun, Z., Zhang, W., & Chen, Q. (2016). A machine vision assisted system for fluorescent magnetic particle inspection of railway wheelsets. *AIP Conference Proceedings, 1706*(1), 150003. https://doi.org/10.1063/1.4940615

-**Wu**, Q., Dong, K., Qin, X., Hu, Z., Xiong, X., & Li, L. (2024). Magnetic particle inspection: Status, advances, and challenges — Demands for automatic non-destructive testing. *NDT & E International, 143*, 103030. https://doi.org/10.1016/j.ndteint.2023.103030

-**Yang**, Y., Yang, Y., Li, L., Chen, C., & Min, Z. (2022). Automatic defect identification method for magnetic particle inspection of bearing rings based on visual characteristics and high-level features. *Applied Sciences, 12*(3), 1293. https://doi.org/10.3390/app12031293

-**Zolfaghari**, A., Zolfaghari, A., & Kolahan, F. (2018). Reliability and sensitivity of magnetic particle nondestructive testing in detecting the surface cracks of welded components. *Nondestructive Testing and Evaluation, 33*(3), 290–300. https://doi.org/10.1080/10589759.2018.1428350